Proceedings of the Canadian Society for Mechanical Engineering International Congress 2021
CSME Congress 2021
June 27-30, 2021, Charlottetown, PE, Canada

INVESTIGATION OF TURBULENT CONVECTIVE HEAT TRANSFER OF MOLTEN SALT FLOW INSIDE A SINGLE-BEND CIRCULAR PIPE

Ehsan Armoudli[1*], Ofelia A. Jianu[1]
[1]Mechanical, Automotive and Materials Engineering, University of Windsor, Windsor, Canada
*armoudl@uwindsor.ca

Abstract—This article investigates the coupled flow and heat transfer behavior of two different nitrate molten salts, i.e., Solar Salt, and Hitec, as they flow in a single-bend of 180 degrees horizontal circular pipe. The internal turbulent flow of these two salts is investigated to heat a part of a high-temperature heat exchanger which will be used in a sustainable thermochemical cycle for hydrogen production. Governing conditions for the high-temperature turbulent flow of molten salts are derived based on the previously published and thoroughly validated articles, applied on the geometry and boundary conditions of the single-bended pipe and then compared with well known, experimentally validated convective heat transfer correlations. This research shows that the bend causes an intense mixing in the flow due to separation. Induced turbulence affects the heat transfer downstream of the bend causing the Nusselt number and the friction factor to increase substantially. Overall, the heat transfer increases at the cost of an increased friction factor and the resultant pressure drops after the bend.

Keywords- Solar Salt; Hitec Salt; Nusselt number; turbulent flow; convective heat transfer; hydrogen production

I. INTRODUCTION

Energy sources are interpreted to be the substantial factors of civilizations flourishment and wellbeing [1]. Global energy consumption is expected to increase by at least 1.4% over the next 20 years [2]. However, due to the adverse effects of overusing the carbon-based fuels, the tendency to shift to more sustainable energy resources has been increased tremendously. Solar, wind, geothermal, tidal, biomass and many other are grouped as sustainable energy sources; however, their commercialization is bonded with their working efficiencies [3]. Due to intermittent and unpredictable nature of sustainable sources, their working efficiency is heavily relying on the methods that can be used for their production storage [4]. Optimal heat and mass transfer include a large portion of total efficiency of most of the storage methods, like hydrogen production. In this context, due to a surge in the working temperature of many sustainable systems, there is a need for high-temperature heat transfer fluids (HTFs) with appropriate flow and heating specifications in temperatures above 400°C. Promising options of HTFs are HITEC Salt (53% KNO_3– 40% $NaNO_2$–7% $NaNO_3$, wt. %) and Solar Salt (40% KNO3–60% NaNO3, mol.%), which both are nitrate-based molten salts [5]. Development of high-temperature heat exchangers is paramount especially for applications in hydrogen and solar energies.

In terms of the reliability of the conventional heat transfer media, Mwesigye and Yılmaz [6] stated that the thermal oil-based heat transfer fluids, which are widely used in the parabolic trough solar collector (PTSC) systems degrade at temperature above 400°C. This is the motive for their benchmark study on ten different heat transfer fluids, namely liquid sodium, lead-bismuth eutectic (LBE), Solar Salt, Hitec, Hitec XL, a ternary salt mixture, a quaternary salt mixture, a new salt mixture, Therminol VP-1, and Dowtherm A, to compare their flow characteristics, stability, thermal and thermodynamic performance. Based on their developed numerical model for a horizontal turbulent flow of mentioned fluids in a circular pipe, which is validated using experimental data from Sandia National Laboratory and Gnielski and Petukuhov correlations, they highlighted that a better heat transfer rate is obtained due to the thinner thermal boundary layer, which is the result of a turbulent flow regime and the effect of higher inlet temperature on density and viscosity of the salts. With a more practical investigation regarding the applicability of such material, Vignarooban et al. [7] listed the expected properties of heat transfer fluids in solar collectors. Their results indicate that HTFs should have low viscosity, high heat storage capacity, high thermal conductivity, low melting point, high boiling point chemical stability, the low vapor pressure at high temperature, low corrosivity with metal alloys, and low cost. Similarly, Krishna et al. [8] classified the HTFs into six groups and compared their flow and thermophysical properties and mentioned the high specific heat, low toxicity flammability, and Industrial availability as other important features of HTFs. Main contributors for selection of the HTFs in this study are [7] and [8].

Some cases of research focused on evaluating the authenticity of existing heat transfer correlations on these new fluid media. Dong et al. [5] investigated the validity of well-known classical correlations and four literature convective heat transfer correlations for a turbulent flow and heat transfer of molten Solar Salt in a circular pipe. They performed experiments for the Reynolds number of between 10,000 and 36,000 and Prandtl number of 4.75 and 8 and found that as the result of the

incline, the bottom of the cylinder has the highest Nusselt and the best heat transfer, while the Nusselt is lowest at the top of the cylinder. They concluded that the differences between the results of experiments and correlations are mainly related to the effect of incline and gravity on the thermal acceleration, which is not considered in the literature correlations, as well as the fact that the correlations are based on the water as the fluid, which is a thousand times lesser in terms of viscosity and density compared to the molten salts. They noted that the most accurate correlation for Nusselt number is the Gnielinski equation [9]. Wu [10] and Dong [11] correlations can also be used within a deviation of ± 20%, which is accepted by the industrial applications.

Qiu et al. [12] experimentally investigated the heat transfer performance and flow friction of four molten salts, i.e. Hitec, Solar Salt, NaF-$NaBF_4$, and FLiNaK in turbulent tube flow under uniform and un-uniform heat flux. They observed that the un-uniform heat flux on the tube will have a minimal influence on the velocity distribution inside the tube, which is caused by buoyancy effect. They asserted that the required Reynolds number of these flows for the industry is between 10^4-10^5 and cannot be covered in experiments due to difficulties with regard to the high-temperature environment. They developed a numerical model as a result of yielding high error (20-25%) between experimental and correlations' result, which returned an error of less than 10%. They showed that the Filonenko's correlation for friction factor will be appropriate for predicting the friction of the salts by having the error of less than ±2%. Finally, they developed a new correlation for Nusselt number based on their simulated data which has an error of less than ±5%.

Using a numerical method in simulating the heat transfer performance of HTFs instead of complicated, time consuming and expensive experimental methods is an appreciated approach especially if we consider the experimental limitations for such high temperature environments. Qiu et al. [12] used a finite volume-based package to solve the governing equations numerically and validated the results with performed experiments for Hitec Salt and well-known empirical correlations. They used the Hansen's, Sider-Tate's, and Gnielinski's correlations for comparing the Nusselt number, with and Filonenko's correlation for friction coefficient. The largest error mentioned to be 25% for Hansen's correlation and 13% for the Sider-Tate's correlation. For the friction coefficient, the error was lower than ±2%. This is proven again in another study by Dong et al. [5] where good agreement is observed between the experimental data and Gnielinski's correlation for Solar Salt in terms of Nusselt number. The same observation is made by Mwesigye and Yılmaz [6] when they compered the numerical results of Nusselt and friction factor with the Gnielinski and Petukhov's correlation.

So far researchers in the current literature have been focused on the type of the HTFs and the prediction of their thermal performance, mainly in simplified geometries. However, the existing heat exchangers purposely include more complexity in the flow regime in order to enhance the overall heat transfer and efficiencies. In this regard, this research investigates the effects of a bended circular pipe on the flow field and thermal behavior of HTFs. Developed numerical model of this study is compared with well-known correlations that can be applied in the simulated condition for Nusselt number and friction factor, to prove the validity of obtained data.

II. METHOD

A. *Modelling of Flow and Heat Transfer in Tube*

The numerical domain that is generated for this study is presented in Fig. 1, dimensions are given in Table 1, and boundary conditions are shown in Table 2. Molten salt flow is a pressure driven flow that enters the tube from the upper pipe inlet section at different mean velocity with fully developed profile, passed through the upper tube, with constant heat absorption, and then the bended section of the tube, and leaves the tube at the lower pipe outlet section. Different inlet Reynolds conditions are presented in Table 3. Material specifications of the molten salts are temperature-variant; therefore, effect of gravity for buoyancy is included in the model.

Also, all of the input Reynolds numbers are well above the laminar threshold, therefore, a RANS approach with K- Ɛ model is used to simulate the turbulent content of the flow using COMSOL Multiphysics.

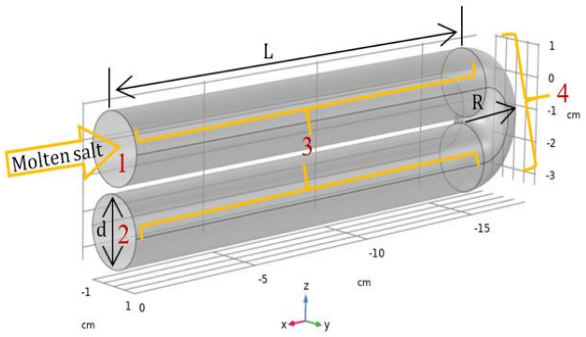

Figure1. Numerical domain and boundary conditions.

TABLE I. Domain Dimensions.

Item	Dimension
d	2.1 cm
R	2.55 cm
L	15.5 cm

TABLE II. Boundary Conditions.

Flow Boundary Conditions		***Heat transfer Boundary Conditions***	
1	Fully developed flow inlet (average velocity)	1	Inflow with constant temperature
2	Pressure outlet	2	Outflow
3	No slip wall	3	Outward constant heat flux boundary
4	No slip wall	4	Thermal insulation

TABLE III. Different Inlet Reynolds Conditions.

Solar Salt		***Hitec Salt***	
Reynolds No.	*Average velocity (m/s)*	*Reynolds No.*	*Average velocity (m/s)*
15000	0.4925	15000	0.399
20000	0.6567	20000	0.532
25000	0.8209	25000	0.665
3000	0.98508	30000	0.798

B. Governing Equations

To completely capture the flow and heat transfer characteristics of the molten salt, Reynolds Averaged Navier - Stokes (RANS) approach is used for modeling the flow. Kays-Crawford model is used for turbulent Prandtl number. The resultant continuity, momentum, and energy equations for a steady and weakly compressible flow are given in (1)-(3):

Continuity equation:

$$\nabla \cdot (\rho u) = 0 \tag{1}$$

Vector equation for conservation of momentum:

$$\rho(u \cdot \nabla)u = \nabla \cdot [-pI + K] + F + \rho g \tag{2}$$

Conservation of energy equation:

$$\rho C_p\big((u \cdot \nabla)T\big) = -(\nabla \cdot q) + \tau : S - \frac{T}{\rho}\frac{\partial \rho}{\partial T}|_p\big((u \cdot \nabla)p\big) + Q \tag{3}$$

where ρ is the density, u is the velocity vector, p is the pressure, K is the viscous stress tensor, F is the volume force vector, C_p is the specific heat capacity at constant pressure, T is the absolute temperature, q is the heat flux vector, Q shows the heat source, and S is the strain-rate tensor which can be computed as:

$$S = \frac{1}{2}(\nabla u + (\nabla u)^T) \tag{4}$$

As suggested in [13] and [14] standard K- Ɛ model is also used with standard wall function to solve the equation sets, which are increased in terms of their unknowns due to the addition of Reynolds stress terms. In (2), K can be written as:

$$K=(\mu+\mu_T)(\nabla u+(\nabla u)^T)-\frac{2}{3}(\mu+\mu_T)(\nabla \cdot u)I-\frac{2}{3}\rho k I \tag{5}$$

where we have:

$$\rho(u \cdot \nabla)k = \nabla \cdot [(\mu + \frac{\mu_T}{\sigma_k})\nabla k] + P_k - \rho\varepsilon \tag{6}$$

$$\rho(u \cdot \nabla)\varepsilon = \nabla \cdot [(\mu + \frac{\mu_T}{\sigma_\varepsilon})\nabla \varepsilon] + C_{\varepsilon 1}\frac{\varepsilon}{k}P_k - C_{\varepsilon 2}\rho\frac{\varepsilon^2}{k} \tag{7}$$

$$\mu_T = \rho C_\mu \frac{k^2}{\varepsilon} \tag{8}$$

$$P_k = \mu_T[\nabla u : (\nabla u + (\nabla u)^T) - \frac{2}{3}(\nabla \cdot u)^2] - \frac{2}{3}\rho k \nabla \cdot u \tag{9}$$

where $C_{\varepsilon 1}$ and $C_{\varepsilon 2}$ are turbulence model parameters. Mentioned equations is discretized over a structured staggered computational grid by considering the effects of density change for the molten salts and the gravity under a steady condition. Except from the turbulent layer, we have two other sub layers, i.e., buffer layer and viscous sub layer, where the K- Ɛ model is not valid.

To avoid high resolution near wall which can increase the computational cost, wall function analytical expressions are used to describe the flow in two sub layers. To obtain the temperature-dependent heat capacity, density, dynamic viscosity, and conductivity of the molten salts, analytic function are defined based on the material specifications presented by [6]. To locate the distance from the wall where these expressions should be applied, a concept referred to as wall lift-off in viscous units, δ_w^+ is defined in the numerical model:

$$\delta_w^+ = \frac{\rho u_\tau \delta_w}{\mu} \tag{10}$$

where u_τ is the friction velocity and δ_w is the wall lift-off. Wall lift-off in viscous units corresponds to the distance from the wall where the logarithmic layer meets to viscous sublayer. After primary simulations, it is concluded that the wall lift-off criteria are met.

C. Computational Domain

Fig. 1 and Table 2 represent the boundary conditions of the numerical domain, which is a part of a heat exchanger used in a hydrogen production cycle. A fully developed velocity profile with different Reynolds numbers is defined for inlet with constant temperature of 823.15 °C. A constant outward heat flux boundary condition is defined for the outer wall layer of upper and lower straight tubes (bend section is thermally insulated). The numerical value for this outward flux is computed based on the available stochiometric and thermal information for the hydrogen production application of this molten salt tube. No slip flow condition is defined at all of the inner wall layer if the tube including the bend section. At the outlet, zero pressure outlet condition is used with backflow suppression because of the known operating condition of such pipes at the outlet which is the atmospheric pressure. A free quad face meshing technique is used along with swept meshing to generate a structured staggered mesh all along the three sub-domains. To improve the resolution of the computational grid near the walls, boundary layer meshing is employed with first layer thickness of 0.007 cm. Total of three different grids with 133238, 279062, and 402752 elements are generated to investigate the mesh independency of the study. Figure 2 shows the result of the mesh independency study by comparing the

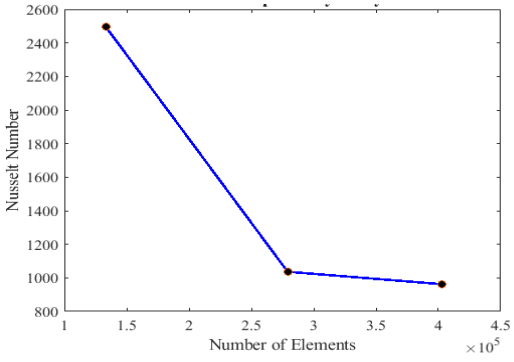

Figure2. Result of Nusselt number for 3 grids.

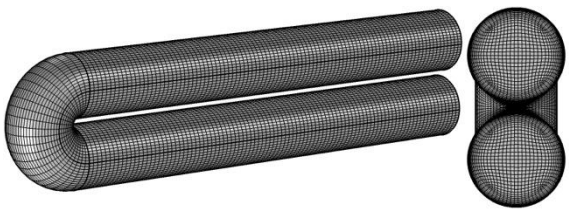

Figure 3. Mesh for preferred grid.

Nusselt for three grids. To compromise between the computational cost (time, hardware, and energy) and the precision of the numerical data, and to minimize the dependency of the results on the numerical grid, the second grid is chosen, which has 279062 elements and is shown in Fig. 3. The difference between the Nusselt number of the third and second grids is not considerable, while the computational cost for the third one is more than twice the second grid.

D. Model Validation

In this case a main result parameter is selected as the indicator and is directly compared against a well-known empirical correlation of the literature [6,9]. Although the inlet condition of the solution is a fully developed velocity profile, the thermal entrance region for these fluids will affect the Nusselt. As mentioned, Gnielinski and well-known Petukhov's correlation for Darcy Weisbach friction factor are used to compare the results for Nusselt and friction factor, respectively. For Gnielinski [9] we have:

$$Nu_D = 0.012(Re_D^{0.8} - 280)Pr^{0.4} \tag{11}$$

For Darcy-Weisbach correlation presented in 12 is used:

$$f = \frac{\Delta P}{\frac{1}{2}\rho u_m^2 \frac{L}{D_{ai}}} \tag{12}$$

and for Petukhov's correlations, Eq. (13) is used:

$$f = (0.79lnRe - 1.64)^{-2} \tag{13}$$

where L is the length over which the flow is intended and D_{ai} is the tube diameter. Such comparison is plotted in the Figs. 4 and 5, and shows proper agreement at all Reynolds numbers. Table 4 shows the relative percent error of both parameters for different Reynolds numbers of Hitec Salt. It can be shown that the relative percent error for both friction factor and Nusselt decreases as Reynolds number increases. Even for small Reynolds numbers, mentioned error is under the acceptable margin which is 20% for industrial applications [10,11].

III. Results and Discussion

After validation of the obtained solutions, the results are presented and discussed in a set of figures in this section. Solution of the flow field is presented in 3-D in Fig. 6. The contours of the velocity magnitude are also provided at several cross sections before and after the bend. It is observed that the flow undergoes a significant change in the velocity as it passes through the bend. This causes a separation of the flow after the bend due to the high inertia and curvature in the bend. Simultaneously, the fluid is accelerated at the outer regions in the cross-section area which is then gradually decreased towards the end of pipe due to the momentum diffusion. Such wake region and induced high velocity motion downstream the bend would cause more turbulence and mixing of the flow, which consequently result in an increased rate of heat transfer.

For assessment of this matter, the velocity and temperature contours are examined at corresponding cross-sections of inlet, immediately before and after the bend and farther after the bend. Figures 7 and 8 show such comparison for Solar Salt and Hitec Salt at Reynolds number 25,000. A separation region in the velocity field is observed after the flow exits the bend, which is in compliance with the flow visualization in Fig. 6. The separation occurs due to the high inertia of the flow and high curvature at the bend. The main effect of the separation is that the flow in the outer side of the bend is accelerated considerably. This accelerated flow will then result in stronger convection, which can increase the local heat transfer. Besides, a mixing effect is caused by the separation that will help the higher centerline temperatures to reach the cold walls faster compared to the straight streamlines. It can be observed that the central streamlines are squeezed towards the outer bend wall, forming a U-shape of the high-velocity region on the outer curvature (Figures 7 & 8, after the bend). Comparing the velocity contours with the corresponding temperature contours shows the effect of flow field mixing on the mixing of the temperature field. By increasing the velocity at the outer region of the curvature, the bend is in fact compressing the thermal boundary layer at the outer region of the bend, which results in higher rate of heat transfer when it leaves the bend. Finally, these bend effects are

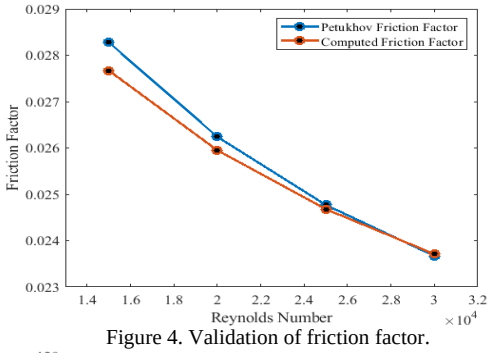

Figure 4. Validation of friction factor.

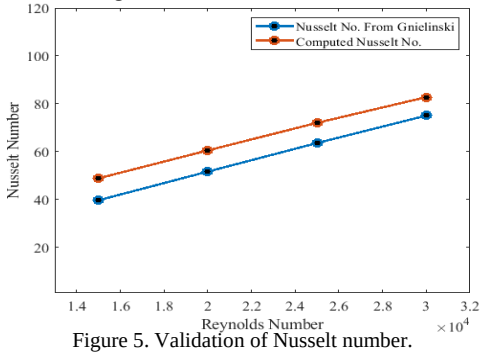

Figure 5. Validation of Nusselt number.

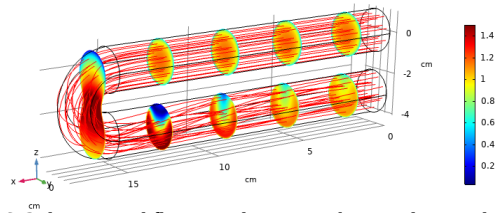
Figure 6. 3-dimensional flow visualization with streamlines and velocity contours for Solar Salt flow at Re 30,000.

TABLE IV. Relative percent error for friction factor and Nusselt number of Hitec Salt.

Reynolds No.	***Relative Percent Error Friction Factor***	***Relative Percent Error Nusselt Number***
15000	2.17	18.76
20000	1.1	14.62
25000	0.33	11.69
30000	0.16	9.31

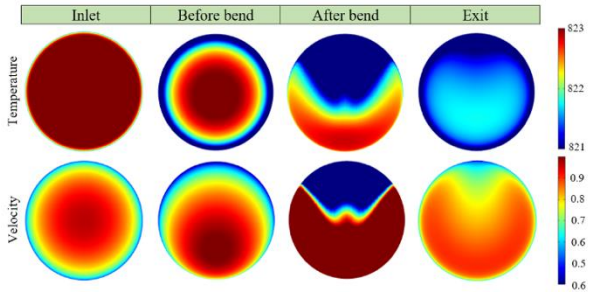

Figure 7. Velocity and temperature contours at cross-section of the inlet of the domain, before and after the pipe and the exit of the domain for Solar Salt at Re 25000.

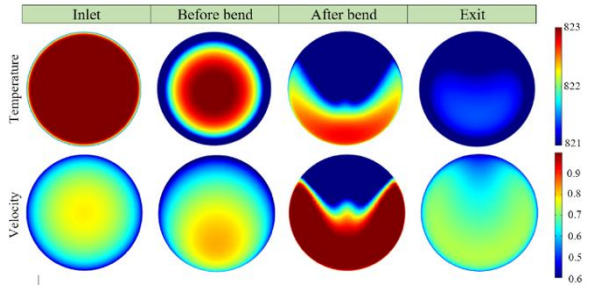

Figure 8. Velocity and temperature contours at cross-section of the inlet of the domain, before and after the pipe and the exit of the domain for Hitec Salt at Re 25000.

visible as the overall more reduction in the fluid temperature downstream the bend in the second pipe, which is an indication of an increased convective heat transfer in the flow.

Comparison of Nusselt is essential for a better insight into the effect of the flow field changes on the enhancement of the heat transfer. Figure 9 shows the variation of Nusselt at two different sections before and after the bend for the Solar Salt and Hitec flows at different Reynolds numbers of 15,000 to 30,000. Calculation of the Nusselt is based on the peripherally averaged temperature of the wall and the temperature of the flow. Therefore, the difference of the velocity field between the inner

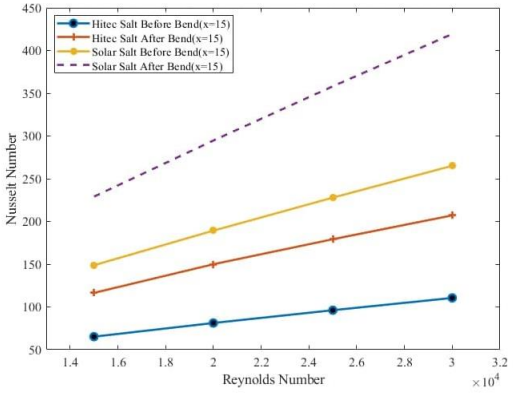

Figure 9. Variation of the local Nusselt number at different Reynolds numbers for Solar Salt and Hitec salt flow.

and outer curvatures of the bend are averaged into the total Nusselt number at that section. This is more pronounced for the section after the bend where the separation of the flow at the inner curvature and acceleration at the outer curvature of the

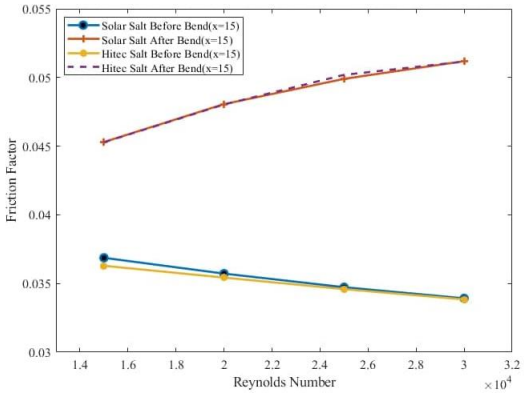

Figure 10. Variation of friction factor at different Reynolds numbers for Solar Salt and Hitec Salt flow.

bend result in different local Nusselt numbers. Comparing the Nusselt before and after the bend for solar salt shows a significant growth from 53% to 60% for different Reynolds numbers. This is actually showing the effect of accelerated flow observed from the bend, and the consequent effects on the boundary layer and temperature changes. Also, at both sections, Nusselt increases at higher Reynolds numbers. This is due to the fact that higher inertia of the fluid flow is capable of enhancing the rate of heat transfer which is a known phenomenon. The Nusselt enhancement after the bend grows at higher Reynolds numbers e.g. for solar salt, it is at 53% at Re 15,000 and grows to 60% at Re 30,000. In other words, the sensitivity of the Nusselt to the Reynolds number is higher after the bend compared to prior to the bend. This is due to the fact that higher inertia results in higher flow deviation at the bend and increased heat transfer at the outer wall. This again emphasizes on the effect of the flow change of the bend on the heat transfer. The same pattern is observed when the other Hitec Salt is the fluid. Figure 9 shows the Nusselt variation against Reynolds number at the same sections before and after the bend at Reynolds numbers of 15,000 to 30,000. The overall Nusselt number of Hitec flow is less compared to the values from Solar Salt. However, the enhancement of Nusselt increased from 68% to 86%.

As another important parameter in design of heat transfer devices, Figs. 10 shows the variation of Darcy- Weisbach friction factor for both salts at different Reynolds numbers and two sections before and after the bend. It is observed that similar to Nusselt number, the friction factor after the bend is also showing an increase at all Reynolds numbers. With a minimum increase of 25% for both salts, this increase can be as high as 51% for Solar Salt at Re 30,000. This increase is due to the fact that deviated flow after the bend compresses the laminar sublayer of the boundary layer to the outer wall, which reduces the boundary layer thickness and increases the drag on the surface of the wall. Moreover, while the friction factor slightly decreases at higher Reynolds numbers before the bend, it shows an opposite trend after the bend. As observed from the Figs. 7 and 8 the region after the bend is highly affected by the wake of the flow separation at the bend. This wake region has two effects: one is the increased drag due to the separated flow after the inner side of the bend and the other is the thinned laminar sublayer at the outer region of the bend, which increases the

drag. The higher inertia of the flow inside the pipe augments these two factors, which is shown in the form of friction factor increase at higher Reynolds numbers. Therefore, the improvement of the heat transfer by the bend comes at the price of increasing the friction and pressure drop in the bended pipe.

IV. Conclusion

The conclusions of this study may be summarized in three categories:

- Velocity and temperature profiles: The bend causes an intense acceleration in the flow. This mixing results from a separation zone and it affects the temperature profile downstream the bend.
- Nusselt number: The bend will increase the Nusselt number considerably due to the increased velocity and turbulence in the flow field.
- Friction factor: The friction factor is relatively constant in the direction of the flow in the upper tube; however, the bend causes separation in the flow and consequently the friction factor is increased for all the cases.

The effect of the bend on increasing the Nusselt number, locally and overall, is the main outcome of this study, as the results will be used in designing a molten salt heat exchanger. However, it is also shown that the bend will induce large temperature gradient immediately after the bend which is not favorable and needs more investigation.

References

[1] H. Ishaq, I. Dincer, and G. F. Naterer, "Multigeneration system exergy analysis and thermal management of an industrial glassmaking process linked with a Cu–Cl cycle for hydrogen production," *International Journal of Hydrogen Energy*, vol. 44, no. 20, pp. 9791–9801, 2019.

[2] U. EIA, *International Energy Outlook 2016. Washington, DC: US Energy Information Administration*. 2016.

[3] T. B. Johansson, H. Kelly, A. K. Reddy, and R. H. Williams, "Renewable energy: sources for fuels and electricity," 1993.

[4] F. Dawood, M. Anda, and G. M. Shafiullah, "Hydrogen production for energy: An overview," *International Journal of Hydrogen Energy*, vol. 45, no. 7, pp. 3847–3869, 2020.

[5] X. Dong, Q. Bi, X. Cheng, and F. Yao, "Convective heat transfer performance of solar salt in inclined circular tube," *Applied Thermal Engineering*, p. 115349, 2020.

[6] A. Mwesigye and İ. H. Yılmaz, "Thermal and thermodynamic benchmarking of liquid heat transfer fluids in a high concentration ratio parabolic trough solar collector system," *Journal of Molecular Liquids*, vol. 319, p. 114151, 2020.

[7] K. Vignarooban, X. Xu, A. Arvay, K. Hsu, and A. M. Kannan, "Heat transfer fluids for concentrating solar power systems–a review," *Applied Energy*, vol. 146, pp. 383–396, 2015.

[8] Y. Krishna, M. Faizal, R. Saidur, K. C. Ng, and N. Aslfattahi, "State-of-the-art heat transfer fluids for parabolic trough collector," *International Journal of Heat and Mass Transfer*, vol. 152, p. 119541, 2020.

[9] V. Gnielinski, "New equations for heat and mass transfer in turbulent pipe and channel flow," *Int. Chem. Eng.*, vol. 16, no. 2, pp. 359–368, 1976.

[10] Y.-T. Wu, C. Chen, B. Liu, and C.-F. Ma, "Investigation on forced convective heat transfer of molten salts in circular tubes," *International Communications in Heat and Mass Transfer*, vol. 39, no. 10, pp. 1550–1555, 2012.

[11] X. Dong, Q. Bi, and F. Yao, "Experimental investigation on the heat transfer performance of molten salt flowing in an annular tube," *Experimental Thermal and Fluid Science*, vol. 102, pp. 113–122, 2019.

[12] Y. Qiu, M.-J. Li, M.-J. Li, H.-H. Zhang, and B. Ning, "Numerical and experimental study on heat transfer and flow features of representative molten salts for energy applications in turbulent tube flow," *International Journal of Heat and Mass Transfer*, vol. 135, pp. 732–745, 2019.

[13] Y. M. Ferng, K.-Y. Lin, and C.-W. Chi, "CFD investigating thermal-hydraulic characteristics of FLiNaK salt as a heat exchange fluid," *Applied Thermal Engineering*, vol. 37, pp. 235–240, 2012.

[14] Z. D. Cheng, Y. L. He, F. Q. Cui, R. J. Xu, and Y. B. Tao, "Numerical simulation of a parabolic trough solar collector with nonuniform solar flux conditions by coupling FVM and MCRT method," *Solar Energy*, vol. 86, no. 6, pp. 1770–1784, 2012.